

See discussions, stats, and author profiles for this publication at: <https://www.researchgate.net/publication/299978959>

# Haematite natural crystals: Non-linear initial susceptibility at low temperature

Article in *Geophysical Journal International* · May 2016

Impact Factor: 2.56 · DOI: 10.1093/gji/ggw134

---

READS

13

2 authors, including:



[S. Guerrero-Suárez](#)

Complutense University of Madrid

8 PUBLICATIONS 11 CITATIONS

[SEE PROFILE](#)

# Hematite natural crystals: non-linear initial susceptibility at low temperature

S. Guerrero Suarez<sup>1</sup>, F. Martín-Hernández<sup>1,2</sup> \*

<sup>1</sup>*Departamento de Física de la Tierra, Astronomía y Astrofísica I,*

*Facultad de Ciencias Físicas, Universidad Complutense de Madrid,*

<sup>2</sup>*Instituto de Geociencias (UCM, CSIC),*

*Facultad de Ciencias Físicas, Universidad Complutense de Madrid, 28040 Madrid, Spain*

## SUMMARY

Several works have reported that hematite has non-linear initial susceptibility at room temperature, like pyrrhotite or titanomagnetite, but there is no explanation for the observed behaviours yet. This study sets out to determine which physical property (grain-size, foreign cations content, domain walls displacements) controls the initial susceptibility. The performed measurements include microprobe analysis to determine magnetic phases different to hematite; initial susceptibility (300 K); hysteresis loops, SIRM and backfield curves at 77 K and 300 K to calculate magnetic parameters and minor loops at 77 K, to analyze initial susceptibility and magnetization behaviours below Morin transition. The magnetic moment study at low temperature is completed with measurements of Zero Field Cooled- Field Cooled (ZFC-FC) and AC-susceptibility in a range from 5 – 300 K. The minor loops show that the non-linearity of initial susceptibility is closely related to Barkhausen jumps. Because of initial magnetic susceptibility is controlled by domain structure it is difficult to establish a mathematical model to separate magnetic subfabrics in hematite-bearing rocks.

**Key words:** Initial susceptibility, Hematite natural crystal, ZFC-FC, AC susceptibility, minor loops, magnetic domains.

## 1 INTRODUCTION

The theory of Anisotropy of Magnetic Susceptibility (AMS) assumes a linear relationship between magnetization and applied field, that is, the initial susceptibility is field-independent (Tarling & Hrouda 1993). This theory is always valid for diamagnetic minerals, and for paramagnetic minerals when the applied field is too small to align the magnetic moments or temperature is high enough to randomize the magnetic moments. In ferromagnetic minerals, this relationship is non-linear and susceptibility varies as a function of temperature and strength of applied field, although, the assumption that the magnetization versus applied field is linear is generally acceptable for fields smaller than 1 mT (Tarling & Hrouda 1993). But there are certain ferromagnetic (s.l.) minerals which display an initial field-dependent susceptibility. For example, pyrrhotite, whose field variation of susceptibility is controlled by grain size (Worm 1991; Worm et al. 1993; de Wall & Worm 1993; Martín-Hernández et al. 2008); titanomagnetite, whose variation of susceptibility is controlled by their  $Ti$  content (Jackson et al. 1998), or hematite, whose controlling factor of susceptibility behaviour is not well understood (Hrouda 2002, 2007; Pokorný et al. 2004).

Field-dependent susceptibility can cause variations in the parameters of the AMS ellipsoid and originates mistaken interpretations in magnetic fabrics studies and rock magnetism (Hrouda 2002; Guerrero-Suarez & Martín-Hernández 2012). The variations of the susceptibility with field strength of some minerals have been modelled mathematically by Hrouda et al. (2006) giving rise to a useful tool to compute separation of magnetic subfabrics (Hrouda 2009; Hrouda & Ježek 2014), identification of magnetic phases (Hrouda et al. 2006; Pokorný et al. 2006) and compositional analysis (Hrouda & Ježek 2014). These models are precise in magnetite-titanomagnetite-bearing samples, but not in hematite-bearing rocks, because the behaviour of initial susceptibility changes from one specimen to another and the physical parameter that controls this behaviour is unknown (Hrouda 2002; Guerrero-Suarez & Martín-Hernández 2012).

Some authors have hypothesized that the differences observed in initial susceptibility of hematite samples are caused by measuring at fields high as those in which magnetization is in the irreversible zone (Hrouda 2002). But Guerrero-Suarez & Martín-Hernández (2012) has recently proposed that the domain orientation or displacements of Bloch walls might explain this phenomenon.

\* Corresponding author: saguerre@ucm.es

The current work aims to seek the mechanism that controls initial susceptibility as a function of field strength. In particular, it will be checked which, among grain size, cations-content or domain wall displacements, is responsible for the variation of susceptibility in the 2 – 450 A/m range.

### 1.1 Hematite at low temperature

Hematite ( $\alpha\text{-Fe}_2\text{O}_3$ ) is one of the most important carriers of remanent magnetization on Earth (Dunlop & Özdemir 2001) and a potential carrier of magnetic anomalies on the surface of Mars (Christensen et al. 2000, 2001; Kletetschka et al. 2000b,a, 2005). It is the totally oxidized member of the Hematite-Wüstite solid solution (Butler 1992) and has a magnetic transition at low temperature named Morin transition ( $T_M \sim 250$  K) (Morin 1950). Above the transition, hematite has a spin-canted structure with a small ferromagnetic moment constrained within the crystal basal plane (Morrish 1994). Below the transition, all spins rotate out of the basal plane, becoming a pure antiferromagnetic mineral with the spins lying along the c-axes (Fuller 1987). The mechanism is well explained by the classical Dzyaloshinsky-Moriya theory (Dzyaloshinsky 1958; Moriya 1960). However, Morin transition is inhibited by many factors, some of them being cation inclusions and defects (Morrish 1994), grain-size (Özdemir et al. 2008) or accumulation of stress (Morrish 1994).

Besides spin-canted remanence, hematite has been reported to exhibit another magnetic moment named defect moment (Dunlop 1971). This moment is responsible for the highly variable magnetic properties of hematite and remains below the Morin transition temperature (Özdemir & Dunlop 2005, 2006; Martin-Hernandez & Hirt 2013). Both moments, defect and spin-canted, are not independent, and a defect moment is necessary to renucleate the spin-canted moment during reheating through the Morin transition (Dunlop & Özdemir 2001). Due to the complex magnetization mechanism and the daily variation of temperature suffered on the red planet and some regions on Earth, magnetization of hematite at low temperatures is of particular interest to understand how it is acquired and the remanence can be modified after repeated cooling-heating cycles (Özdemir et al. 2008).

In this work, rock magnetic measurements have been realized at temperature below Morin transition (77 K), where domains should have disappeared since hematite should behave as a pure antiferromagnet, unless the transition is inhibited or the sample has a defect moment. Cycling through the Morin transition is not recommended as a method of domain structure cleaning because if the sample has defect moment, this one enhances at the expense of spin-canted moment (Dunlop & Özdemir 2001). But any irreversible change in the domain configuration caused by cycling through  $T_M$  may be reflected in the behaviour of initial susceptibility (de Boer et al. 2001). To study the magnetic moment at low temperature, ZFC-FC magnetization curves and AC-susceptibility measurements have been made in the 5 – 300 K range.

## 2 MATERIALS AND METHODS

Several factors have been analyzed like possible controllers of the initial susceptibility behaviours reported in hematite by Guerrero-Suarez & Martín-Hernández (2012). The studied parameters are grain size, magnetic phases different to hematite, magnetic parameters and domain wall displacements. All measurements in hematite natural crystals have been carried out within the basal plane.

### 2.1 Sample description

Two types of hematite natural samples have been analyzed: crystals and powder fractions. The crystal samples are from Minas Gerais (Brazil) and are labelled as 1A, 4A, 8A, 17B, 2E, 4E, 1G and 4N. These samples are irregularly-shaped specimens with approximately 4 mm lengths. The specimens labelled by the same letter, like 1A, 4A and 8A indicate that they have been extracted from the same larger crystal. These samples have been selected because exhibit the three initial susceptibility behaviour reported by Guerrero-Suarez & Martín-Hernández (2012).

Initial susceptibility at room temperature, in a field range from 2 up to 450 A/m, has been measured on a KLY-4S Kappabridge susceptometer manufactured by AGICO (Brno, Czech Republic) (Pokorný et al. 2004). The measurements were made in the laboratory of Paleomagnetism at Universidad Complutense de Madrid (Spain). Other twin specimens coming from the same larger samples have already been reported previously elsewhere (Guerrero-Suarez & Martín-Hernández 2012; Martín-Hernández & Guerrero-Suárez 2012).

The powder fractions have been analyzed to determine the influence of grain size as a controlling factor of the initial susceptibility. This set of samples belong to the personal collection of prof. M. J. Dekkers. They are labelled as LH4, LHC (of unknown origin) and LH6 (Hellivara, Lapland), have known grain-sizes and were previously studied by Harstra (1982); Dekkers (1988); de Boer & Dekkers (2001); de Boer et al. (2001).

### 2.2 Compositional analysis

Quantification of different existing phases have been determined by microprobe analysis. Microprobe analysis of 4A, 2E, 1G, 4N and 8A crystal samples has been carried out in a superprobe JXA-8900M manufactured by JEOL company (Tokyo, Japan) at ICTS Centro Nacional de Microscopía Electrónica (Universidad Complutense de Madrid, Spain). This measurement indicates the amount in % of the following phases:  $Al_2O_3$ ,  $MnO$ ,  $TiO_2$ ,  $Cr_2O_3$ ,  $Fe_2O_3$  and  $SnO_2$ . X-ray diffraction and mass spectrometry measurements on twin crystals specimens can be found elsewhere (Guerrero-Suarez & Martín-Hernández 2012; Martín-Hernández & Guerrero-Suárez 2012). Similar characterization (microprobe

analysis, x-ray diffraction, optical microscopy) was carried out in grain size fractions by other authors and further compiled by de Boer & Dekkers (2001).

### 2.3 Rock Magnetic crystal characterization

Classical rock magnetic characterization of the sample's basal plane has been determined in a Vibrating Sample Magnetometer (VSM) manufactured by Princeton Measurements Corporation (Princeton, NJ, USA). The measurements were made at Institute for Rock Magnetism (University of Minnesota, USA).

Measurements were carried out at two temperatures, 77 K and 300 K, in fields up to 1.5 T. The magnetic properties of the crystals include the three parameters derived from hysteresis loops ( $M_r$ ,  $M_s$ , and  $B_c$ ) and acquisition of saturation isothermal remanent magnetization curves (SIRM) and the coercivity of remanence obtained ( $B_{cr}$ ) from further static demagnetization (backfield SIRM).

Additional thermomagnetic curves on twin specimens of hematite natural crystals can be found elsewhere (Martin-Hernandez & Guerrero-Suárez 2012).

### 2.4 Minor loops

The variation of the initial susceptibility with applied field at 77 K has been derived from a set of minor loops measured on a VSM at Institute for Rock Magnetism (University of Minnesota, USA). Magnetization was measured with an averaging time of 0.1 s and a field increment of  $10^{-6}$  T.

Initial induced magnetization can be reasonably described by the Rayleigh law, which characterizes a minor loop by a quadratic expression (Néel 1953; Borradaile & Jackson 2004; Bozorth 1993):

$$M = (\chi_{init} + \alpha H_0)H \pm \alpha/2(H_0^2 - H^2) \quad (2.1)$$

where the negative sign applies to the ascending branch of the minor loop and the positive sign to the descending branch.  $H_0$  is the maximum applied field for every individual loop,  $\chi$  is the initial susceptibility and  $\alpha$  is the Rayleigh coefficient. Magnetization curve have been fitted into a second order polynomial in order to calculate the value of  $\chi$  at different values of  $H_0$ .

Minor loops at 77 K are also illustrative of the magnetization process. Hysteresis bellow the Morin transition indicates a magnetic moment at low temperatures. Wall domain displacements can also be recognised by abrupt changes in these magnetization curves.

### 2.5 Low temperature remanence magnetization

The magnetic moment observed at low temperature can be analyzed by DC and AC measurements. DC measurements like ZFC-FC, give information about the static moment or remanence. In this study, the

remanence (SIRM) was measured on warming from 5 K to 300 K starting from two initial states, field-cooled (FC) in 2.5 T field and zero-field-cooled (ZFC), from 300 K to 5 K after which a saturating field of 2.5 T was imparted. The measurements were made on a MPMS susceptometer manufactured by Quantum Design at Institute for Rock Magnetism (University of Minnesota, USA).

## 2.6 AC susceptibility

AC susceptibility is an effective tool for characterizing minerals owing to the time dependence of the induced moments and magnetization dynamics. The magnetization behaviour at low frequencies follows the  $M(H)$  curve that would be measured in a DC experiment. At higher frequencies, the magnetization curve shows the dynamic effects in the samples.

The AC magnetic susceptibility measurements yields two quantities: the real or in-phase susceptibility ( $\chi'$ ) and the imaginary or out-phase susceptibility. When the maximum applied field is very small, the quadratic terms in 2.1 can be discarded and the initial susceptibility would be:

$$\chi' = \chi_{init} + \alpha H_0 \quad (2.2)$$

where  $\chi'$  is named in-phase susceptibility. The out-of phase or imaginary component ( $\chi''$ ), would be defined by:

$$\chi'' = 4\alpha H_0 / 3\pi \quad (2.3)$$

Both  $\chi'$  and  $\chi''$  are very sensitive to thermodynamic phase changes. In particular, the in-phase susceptibility informs about the dissipative processes and, as such, it has been classically fitted into an Arrhenius equation that relates frequency and activation energy (Özdemir et al. 2009; Church et al. 2011). An estimation of the activation energy can be obtained of the relaxation phenomenon ( $E_a$ ):

$$\tau = \tau_0 \exp \frac{E_a}{\kappa_B T} \quad (2.4)$$

where the relaxation time,  $\tau = (2\pi f)^{-1}$ , is obtained from the measurement frequency,  $f$ .  $\kappa_B$  is the Boltzmann constant and  $\tau_0$  is the characteristic attempt time. For a given susceptibility, the slope of the Arrhenius plot, where  $\ln(\tau)$  is represented as a function of  $1/T$ , yields  $E_a/\kappa_B$  and the intercept  $\ln(\tau_0)$ .

The frequency-dependent susceptibility was measured with a Quantum Design (Magnetic Properties Measurement System, MPMS) cryogenic susceptometer (San Diego, CA, USA) at Institute for Rock Magnetism (University of Minnesota, USA). The measurements were made between 5 and 300 K, in frequencies of 1, 3, 10, 30, 100, 300 and 1000 Hz.

**Table 1.** Summary of amount of cations  $Al_2O_3$ ,  $MnO$ ,  $TiO_2$ ,  $Cr_2O_3$ ,  $Fe_2O_3$  and  $SnO_2$  in % for samples 8A, 4N, 4A, 2E and 1G.

Samples	$Al_2O_3$		$MnO$		$TiO_2$		$Cr_2O_3$		$Fe_2O_3$		$SnO_2$
	Mean	std	Mean	std	Mean	std	Mean	std	Mean	std	Mean
8A	0.028	0.013	0.030	0.023	3.22	0.22	0.122	0.033	96.34	0.69	0.020
4N	0.029	0.021	0.051	0.010	4.83	0.21	0.280	0.039	94.59	0.36	0.017
4A	0.051	0.008	0.032	0.026	2.73	0.06	0.088	0.043	96.76	0.31	0.042
2E	0.033	0.022	0.042	0.019	5.01	0.32	0.275	0.036	93.87	0.23	0.018
1G	0.017	0.012	0.021	0.011	2.93	0.32	0.107	0.042	95.68	0.56	0.011

### 3 RESULTS

#### 3.1 Microprobe compositional analysis

Natural hematite grain-sizes fractions were investigated by Harstra (1982) and further compiled by de Boer & Dekkers (2001). The grain-size fractions were characterized using microprobe analysis (chemical composition), x-ray diffraction (unit-cell parameters) and optical microscopy (shape and lamellar twinning) (Table 1 from (de Boer & Dekkers 2001)). Composition is similar between localities, with mayor abundance of  $Fe_2O_3$  ( $\sim 98\%$ ) and minor phases  $TiO_2$  ( $\sim 0.1 - 0.5\%$ ),  $Al_2O_3$  ( $\sim 0.6\%$ ) and  $Cr_2O_3$  ( $\sim 0.25\%$ ).

The natural crystals have been characterized using microprobe analysis. The results summarized in Table 1, indicate that  $Fe_2O_3$  is the major phase with a minimum value of 94% in sample 2E and a maximum value of 97% in sample 4A. These samples have relevant  $TiO_2$  abundances and  $Cr_2O_3$ . The maximum value of  $TiO_2$  is 5% in samples 2E and 4N and the minimum value is 3% for the rest of samples. The minimum of  $Cr_2O_3$  is 0.1% for sample 1G and the maximum value is 0.3% for sample 4N. Although  $Cr_2O_3$  is unusual in hematite crystals from other localities, has been reported in Minas Gerais by many authors (Morrish 1994).  $MnO$ ,  $Al_2O_3$  and  $SnO_2$  are residual in composition (Table 1).

#### 3.2 Initial susceptibility measurements

##### 3.2.1 Grain-size fractions

The initial susceptibility ( $\chi_{init}$ ) as a function of field strength ( $H$ ) in the  $2 - 450 A/m$  range is shown in Fig. 1 for eight grain-size fractions, which correspond to three different samples LH4, LH6 and LHC. The grain-size fractions range between 10 and  $150 \mu m$  and all of them are PSD or MD (Harstra 1982). The initial susceptibility behaviour is constant for the whole range of applied fields in these samples, except for the largest grain-size fraction of LHC, whose susceptibility increases linearly ( $\sim 4\%$ ) between 2 and  $450 A/m$ . The break in slope at  $350 A/m$  showed in all of these fractions has

an instrumental origin owing to the autoranging of the pick-up unit according to the measurement experience.

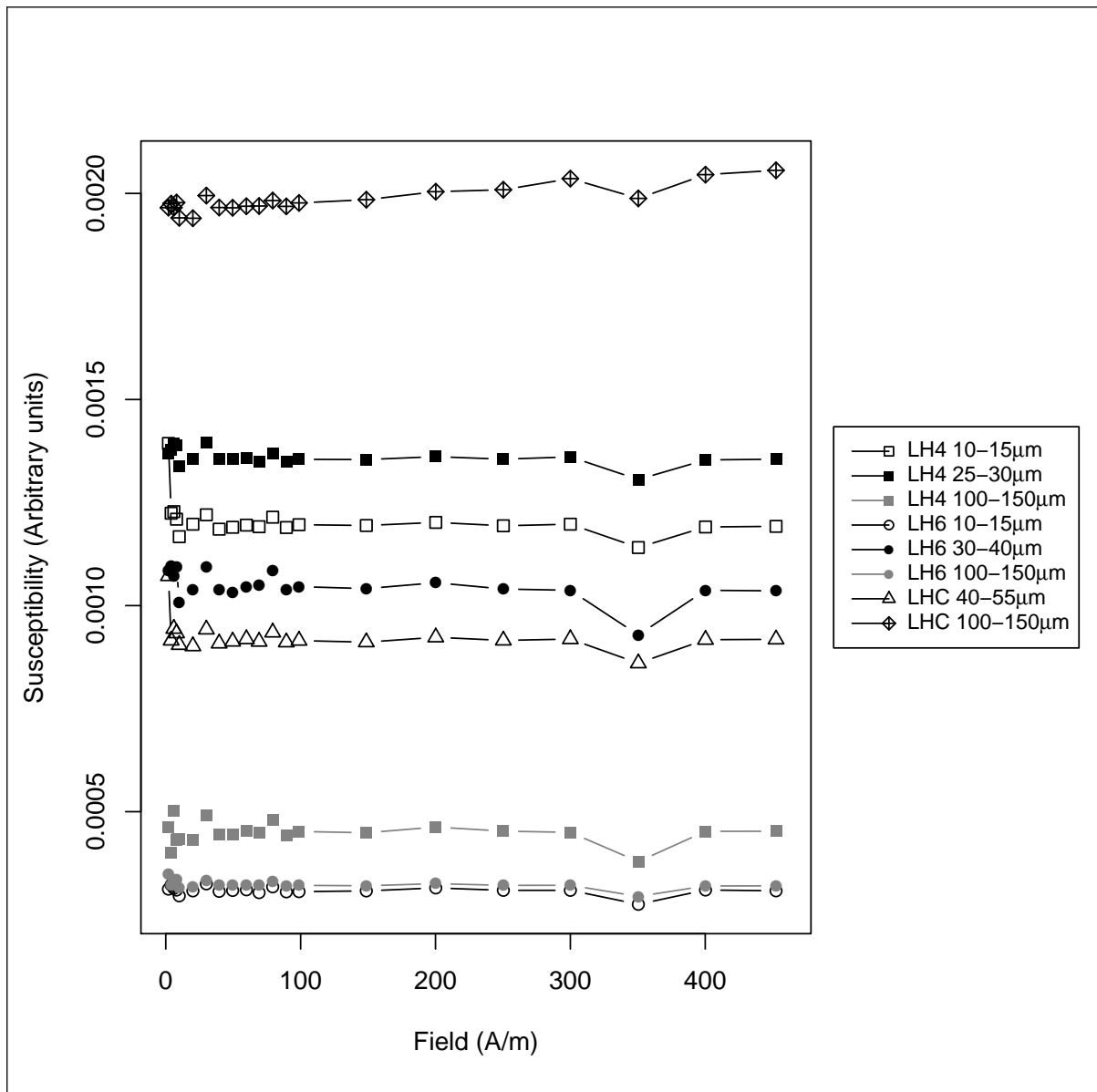


**Figure 1.** Initial susceptibility versus field runs for grain-size fractions natural hematites, from 10 up to 150  $\mu\text{m}$ .

### 3.2.2 Natural crystal samples

The  $\chi_{init}$  vs  $H$  curves obtained for eight crystal samples at room temperature are shown in Fig. 2. The maximum value of susceptibility ranges between 0.2 – 0.9 SI, except sample 17B whose maximum susceptibility is one order of magnitude less, 0.02 SI. Each of these curves can be classified as one of the three categories in hematite natural crystals, as already reported by Guerrero-Suarez & Martín-Hernández (2012). In the first type (i), the samples 17B, 8A, and 1G show a linear increase of  $\chi_{init}$  vs  $H$  in the whole range of applied fields (up to 450 A/m). The second type (ii), samples 4A, 2E and 4N, shows a sudden change in slope. Sample 4A has two changes in slope at 100 and 250 A/m. Sample 2E

also has two changes in slope but at 20 and 200 A/m and the sample 4N at 20 and 250 A/m. In the third type (iii), the samples 4E and 1A, exhibit breaks in slope too, but the slope change from being positive to negative. Sample 4E has this inflection point at 200 A/m, from this field value up to 450 A/m, the susceptibility value decreases  $\sim 12\%$ . Sample 1A has the inflection point at 300 A/m, but susceptibility drop is slightly ( $\sim 4\%$ ).

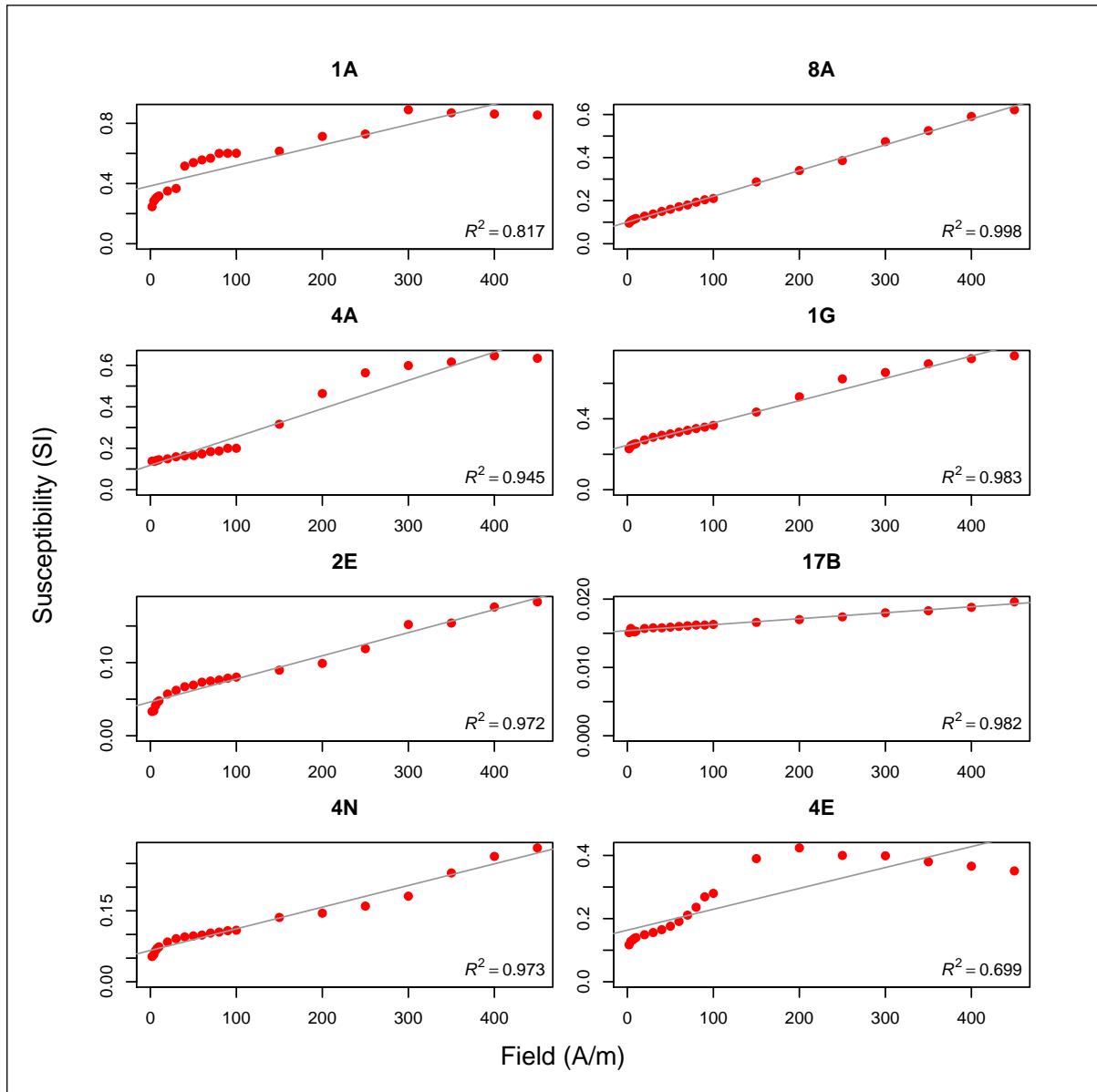


**Figure 2.** Initial susceptibility vs field runs for hematite natural crystals in the range from 2 to 450 A/m, at room temperature.

Fig. 3 shows the  $\chi_{init}$  vs  $H$  behaviour at 77 K for the same eight crystal samples displayed in Fig. 2 at room temperature. The  $\chi_{init}$  at 77 K is computed as the linear term of the  $M(H)$  curve at the end of the minor loops of magnetization. The error bars have been derived from the uncertainties of the slope in the magnetization curves at 95% fiducial limit. In most of the samples, error bars are larger at fields smaller than 100 A/m, indicating that the measurement is less precise at low fields. Figs. 2 and 3 show that there is a big difference between the maximum value of susceptibility at 300 K and at 77 K, except in sample 1A. Maximum susceptibility decreases  $\sim 33\%$  at 77 K in samples 4A, 1G and 4E, one order of magnitude less in samples 2E and 17B, and two orders of magnitude less in samples 8A

and 4N. Fig. 3 shows that the linear fitting to the measured points is better in samples 8A, 1G, 17B, 2E and 4N. In the case of samples 17B, 2E and 4N, the fitting does not exclude a constant behaviour for initial susceptibility. Sample 8A has a linear behaviour and sample 1G presents a change in slope at  $250 \text{ A/m}$ . Samples 1A, 4A and 4E display more than one change in slope for the whole range of applied field ( $2 - 450 \text{ A/m}$ ).

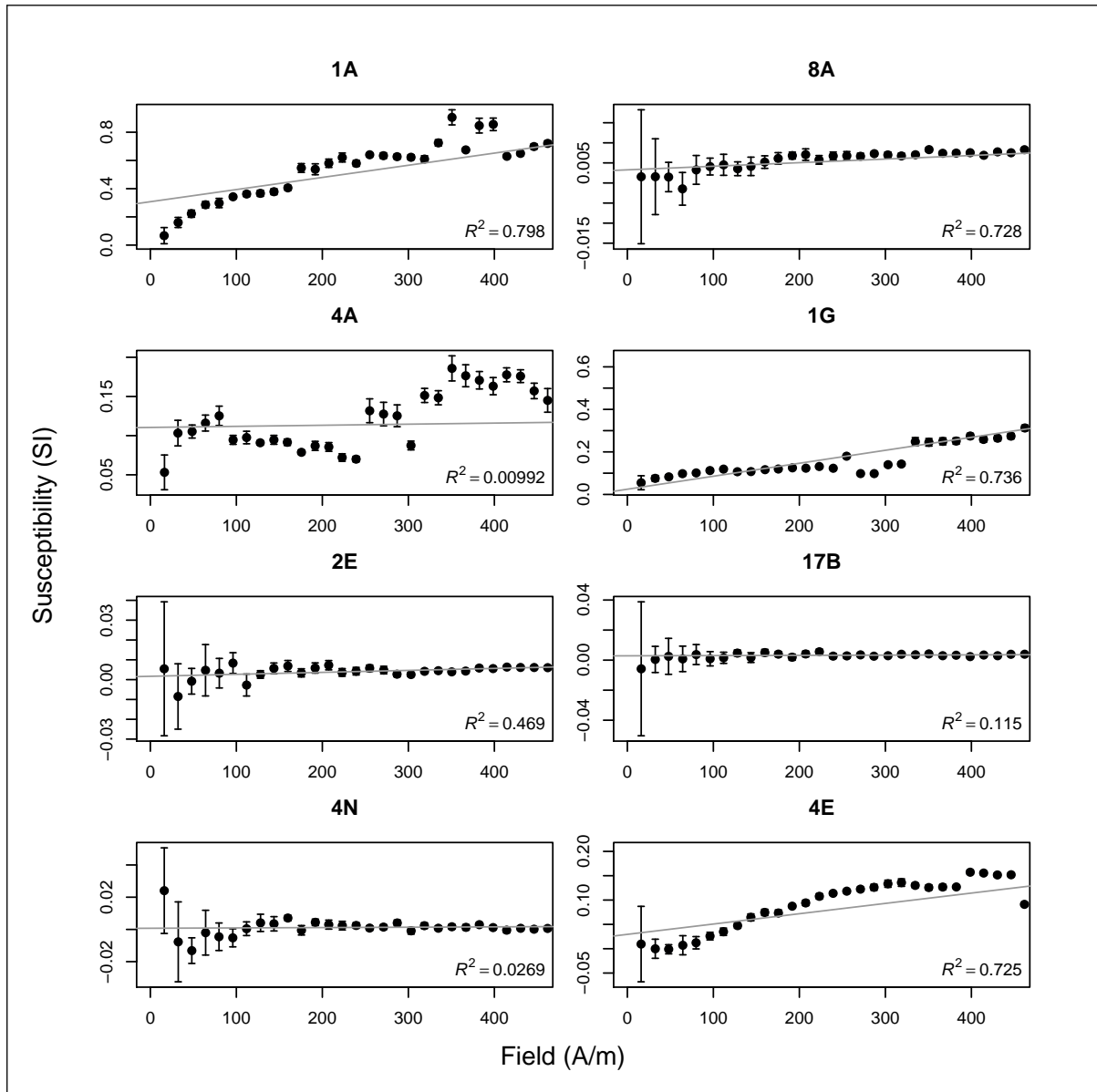


**Figure 3.** Initial susceptibility, derived from minor loops, vs field runs for hematite natural crystals in the range from 2 to 450 A/m, at low temperature (77 K).

### 3.3 Rock magnetic parameters

Classical rock magnetic parameters derived from hysteresis loops, SIRM and back-field, obtained at 300 K and 77 K, are compiled in Table 2 and summarized in the Day plot of Fig. 4 (Day et al. 1977). At 300 K, only the sample 17B has a  $M_r/M_s$  ratio near 0.75, interpreted as a triaxial-dominated anisotropy (Dunlop & Özdemir 2007; Martin-Hernandez & Guerrero-Suárez 2012). The rest of the samples have a  $M_r/M_s$  ratio smaller than 0.5, limit value interpreted as a uniaxial-dominated anisotropy (Dunlop & Özdemir 2001).  $M_r/M_s$  ratios below 0.5 have already been reported for hematite natural

**Table 2.** Magnetic parameters derived from hysteresis loops and backfield SIRM for hematite natural crystals at both temperatures, 300 and 77 K. Also the antiferromagnetic susceptibility.

Sample	$B_{cr}$ (mT)	$B_c$ (mT)	$M_s$ ( $\text{Am}^2/\text{kg}$ )	$M_r/M_s$	$\chi_{ant}$ (SI)	T (K)
17B	33	30	0.283	0.71	$2.37 \cdot 10^{-7}$	77
17B	25	14	0.393	0.65	$2.66 \cdot 10^{-7}$	300
1A	3	4	0.404	0.38	$2.75 \cdot 10^{-7}$	77
1A	3	2	0.433	0.23	$2.53 \cdot 10^{-7}$	300
1G	3	4	0.346	0.43	$2.24 \cdot 10^{-7}$	77
1G	2	2	0.482	0.20	$2.44 \cdot 10^{-7}$	300
2E	19	17	0.286	0.74	$3.49 \cdot 10^{-7}$	77
2E	6	7	0.395	0.30	$2.96 \cdot 10^{-7}$	300
4A	3	2	0.180	0.27	$1.19 \cdot 10^{-7}$	77
4A	3	3	0.475	0.30	$2.32 \cdot 10^{-7}$	300
4E	5	5	0.334	0.48	$2.72 \cdot 10^{-7}$	77
4E	2	2	0.455	0.16	$2.52 \cdot 10^{-7}$	300
4N	7	8	0.171	0.65	$1.93 \cdot 10^{-7}$	77
4N	2	3	0.445	0.33	$2.93 \cdot 10^{-7}$	300
8A	4	4	0.193	0.51	$1.37 \cdot 10^{-7}$	77
8A	2	2	0.225	0.23	$1.43 \cdot 10^{-7}$	300

crystals measured within the basal plane and natural bearing rocks (Martin-Hernandez & Guerrero-Suárez 2012; Martin-Hernandez & Hirt 2013; Peters & Dekkers 2003).

At 77 K,  $M_r/M_s$  increases in all samples except in sample 4A, where the difference of magnetization ratios at both temperatures is 0.03, giving rise to an almost constant ratio. At this temperature, magnetization ratio of samples 2E, 17B and 4N is nearly laying on the triaxial area, and the ratio of samples 4E and 8A is almost in the uniaxial area, but the ratio of samples 1G and 1A is smaller than 0.5.  $B_{cr}/B_c$  decreases. Sample 2E coercivity ratio can be explained by a lack of precision.

Saturation magnetization of all samples is higher at 300 K than at 77 K and coercivity of remanence for samples 17B, 2E and 4N is significantly higher at 77 K than at 300 K. The antiferromagnetic susceptibility, or susceptibility above the saturation of the ferromagnetic phase, for all samples has the same order of magnitude for both temperatures (Morrish 1994).

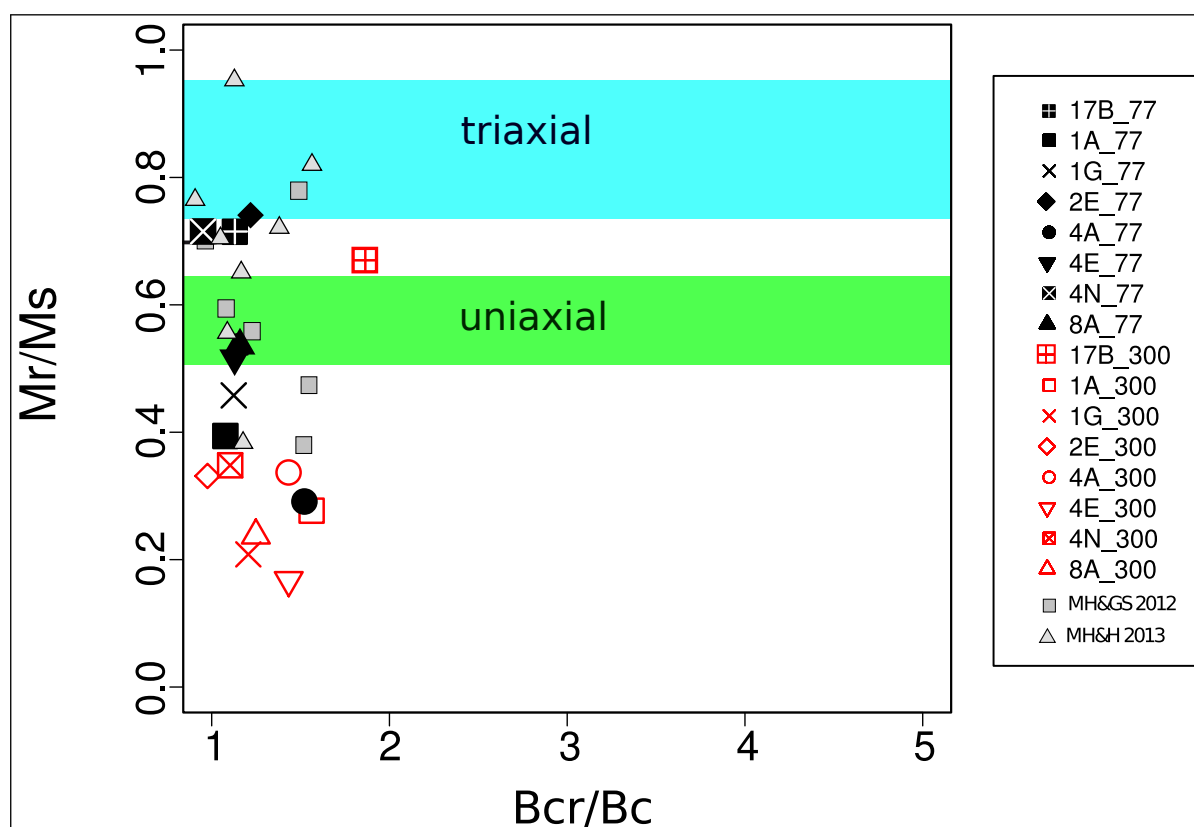


**Figure 4.** Day plot for the hematite natural crystals (Day et al. 1977). Open symbols represent measurements at room temperature and full symbols correspond to measurements at 77 K. Compilation of previously reported values is also shown (gray squares (Martin-Hernandez & Guerrero-Suárez 2012) and gray triangles (Martin-Hernandez & Hirt 2013)).

### 3.4 Minor loops

Besides initial susceptibility, Barkhausen jumps can be obtained from minor loops. Equation 2.1 describes the relationship between magnetization and applied field within the Rayleigh region (Bozorth 1993) Fig. 5 displays the magnetization gradient (Barkhausen jumps) as a function of applied field. Samples 8A, 17B and 4N do not show magnetization gradients larger than signal noise. Sample 1G and 4E have significant jumps above 250 A/m and sample 4A below 250 A/m.

### 3.5 ZFC-FC remanence

The ZFC-FC curves are displayed in Fig. 6. These graphs show two types of the remanent magnetization in the basal plane as a function of temperature (5 – 300 K). Most of the samples have a decrease in magnetization with increasing temperature, except sample 4N and 2E (Fig. 6 and Supplementary material). These two samples (4N and 2E) have constant magnetization in FC warming and experiment recovery of remanence in ZFC warming, at temperature higher than 30 K. There are two common features in all samples: the absence of a clear Morin transition and a remanence loss in the warming curve at about  $\sim 20$  K.

Morin transition, which is exclusive of hematite (Morin 1950) is characterized by a magnetization drop when the temperature goes below  $\sim 250$  K. In this set crystals, only samples 2E and 4N show a magnetization decrease in ZFC until  $\sim 30$  K (Fig. 6 and Supplementary material). However this decrease is not a typical magnetization drop in hematite. Samples 17B and 8A exhibit an inflection point in the magnetization at temperature around 200 K, but with opposite trend, magnetization increases slightly below 200 K (Fig. 6 and Supplementary material). The rest of samples do not show any special feature around the theoretical Morin temperature (Supplementary material).

All samples show a sharp drop of magnetization in FC and slight drop of magnetization in ZFC in the range from 5 to  $\sim 20$  K. During this range of temperature, the differences between  $M_{FC}$  and  $M_{ZFC}$  are larger and tend to vanish with increasing temperature, so above 20 K ZFC-FC curves of most of the samples are completely reversible. The irreversibility temperature ( $T_{irr}$ ) reported in Table 3, is calculated as the temperature (in warming) at which the value of  $(M_{FC} - M_{ZFC})/M_{FC}$  is less than 1%. Almost all samples have a  $T_{irr} \sim 20$  K, except samples 17B, 4N and 2E, whose  $T_{irr}$  are 25 K, 40 K and 255 K, respectively. Sample 1A has another irreversibility region between 160 – 200 K and sample 8A shows irreversibility above 200 K.

Another important parameter derived from ZFC curves is  $T_p$ , the temperature at which the ZFC curve has an inflection point (cusp) or maximum. The  $T_p$  range is between 25 – 35 K (Table 3).

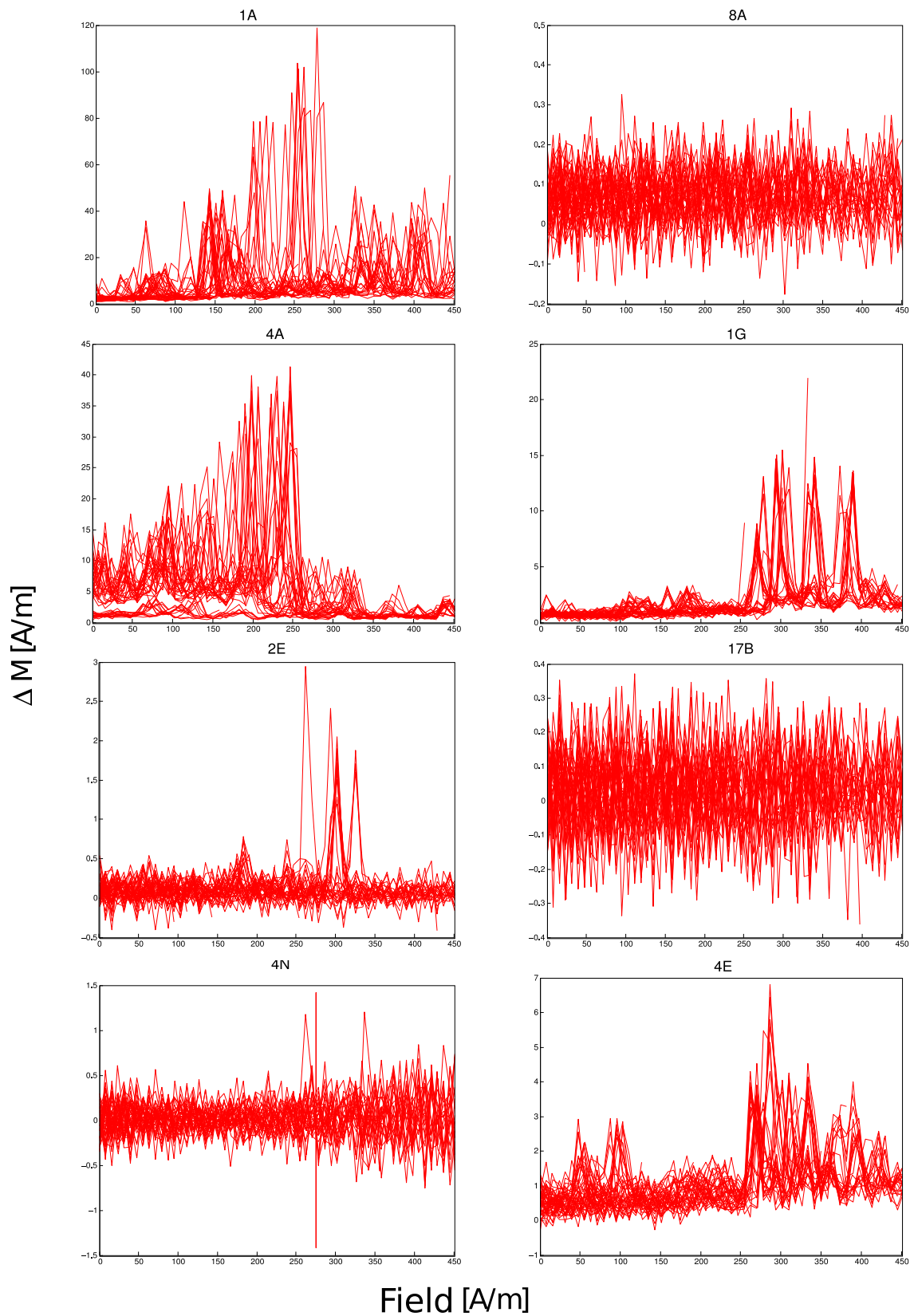
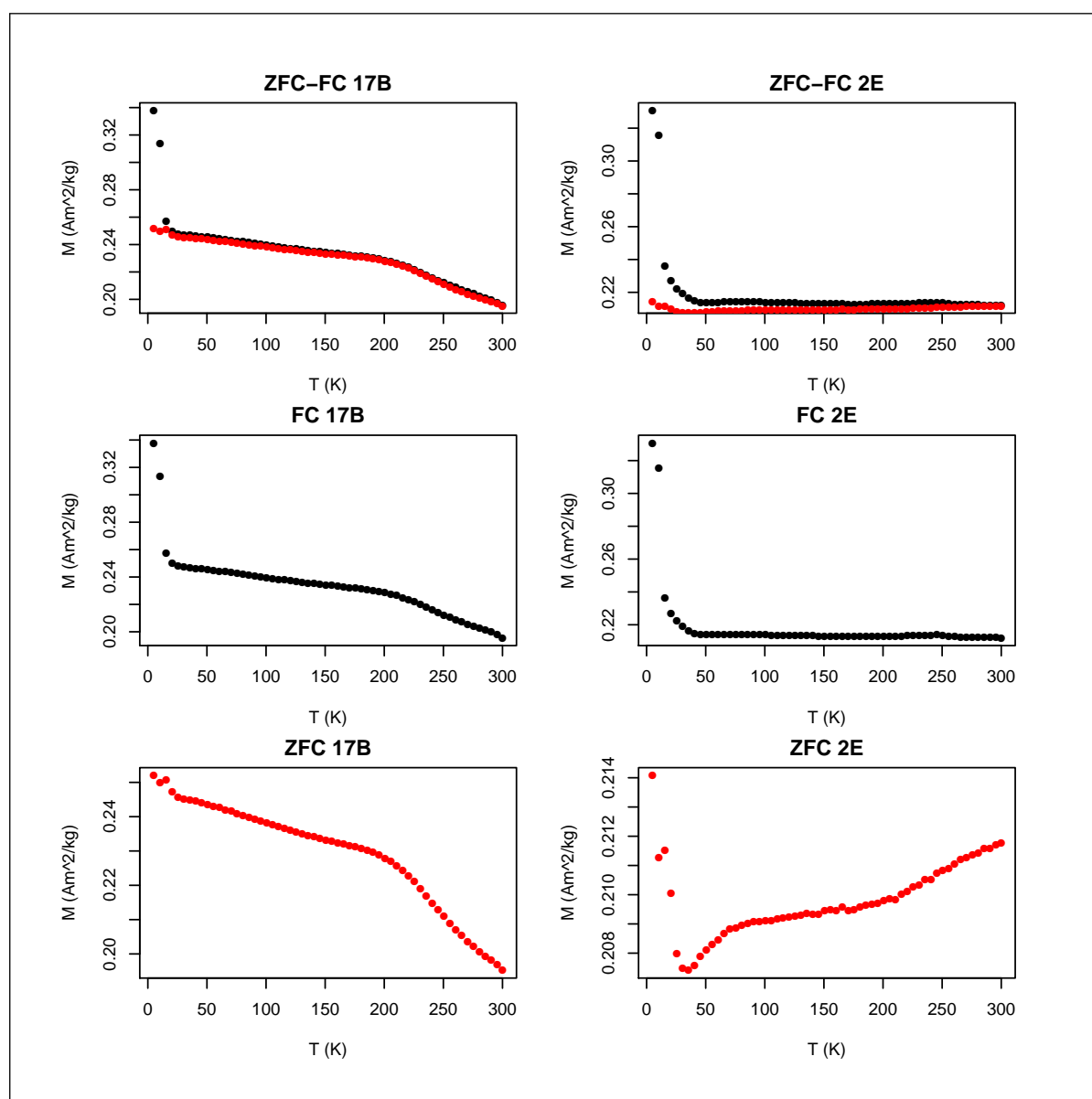


Figure 5. Barkhausen jumps at 77 K



**Figure 6.** ZFC-FC from 5 to 300 K for hematite natural crystals. a) sample 17B and b) sample 2E.

### 3.6 AC susceptibility

The in-phase susceptibility for the 5 – 300 K temperature range and the corresponding Arrhenius plot are summarized in Fig. 7. Specific values of the activation energy ( $E_a$ ) and relaxation time are summarized in Table 3. Two phenomena can be distinguished in Fig. 7: a relaxation phenomenon and a phase transition.

Relaxation phenomenon starts around 20 K for all samples and, depending on the frequency, extends up to a maximum temperature of about 150 K in samples 1A and 4E (Supplementary material). The samples with lower frequency dependence (17B, 4N and 2E) have a smaller relaxation time with

**Table 3.** Summary of Activation energy ( $E_a$ ), relaxation time ( $\tau_0$ ), irreversible temperature ( $T_{irr}$ ) and inflection point temperature ( $T_p$ ) for hematite natural crystals.

Sample	$E_a$ (eV)	$\tau_0$ (s)	$T_{irr}$ (K)	$T_p$ (K)
1A	0.055	$2.6 \cdot 10^{-7}$	21.7	36.6
4A	0.054	$1.5 \cdot 10^{-7}$	21.6	36.6
8A	0.053	$1.2 \cdot 10^{-7}$	20.6	25.5
17B	0.050	$1.1 \cdot 10^{-9}$	25.5	25.5
2E	0.095	$5.8 \cdot 10^{-10}$	255.5	35.6
4E	0.054	$1.7 \cdot 10^{-7}$	20.6	30.6
1G	0.046	$4.5 \cdot 10^{-8}$	20.6	35.5
4N	0.053	$1.8 \cdot 10^{-9}$	40.5	30.6

values lower than  $10^{-8}$  s (Table 3) and a  $\chi''$  value smaller than  $10^{-8}$  m<sup>3</sup>/kg, except the sample 2E, whose  $\chi''$  is bigger. However, despite the differences in the characteristic relaxation time, the activation energies are very similar, with a mean value of 0.053 eV, similar to the activation energy of hematite nanoparticles reported in the literature (Tadić et al. 2007), except for sample 2E that has an activation energy value of 0.095 eV. In the vicinity of the Morin transition a small increase in  $\chi'$  and in  $\chi''$  is observed in samples 1A, 8A, 4A, 17B, 4E and 2E. This cusp is a typical feature of susceptibility parallel to the basal plane (Morrish 1994) at the Morin transition.

#### 4 DISCUSSION

The non-linear behaviour of the initial susceptibility on hematite with increasing field strength is a behaviour reported in the recent years. Other common minerals in nature, like titanomagnetite or pyrrhotite, show a dependence of initial susceptibility vs field with the amount of  $Ti$  and the grain size, respectively ([Jackson et al. 1998](#); [Worm et al. 1993](#)). In hematite, some authors have hypothesized that the non linear behaviour of susceptibility is related to measurements made in fields higher than the coercivity or outside the Rayleigh zone ([Hrouda 2002](#)). In the current study, the influence of magnetic phases, grain size, magnetic parameters and domain walls displacements on the initial susceptibility behaviour of hematite samples has been analyzed.

The major phase observed by microprobe analysis different to  $Fe_2O_3$ , in hematite crystal samples is  $TiO_2$ , but it seems an unlikely dominant parameter controlling initial susceptibility. Data are contradictory in this respect. While sample 4A is non linear and has the lowest  $Ti$  content, sample 8A has the most linear behaviour and still a “moderate”  $Ti$  content with respect to other samples (Table 1 and Fig. 2).

Specific experiments on grain sized fractions exclude a possible influence of the physical dimension of grains (Fig. 1). The initial magnetic susceptibility is constant for all the analyzed samples, except for LHC100-150 what shows a linear increase (Fig. 1). In this work, the strong variation of initial susceptibility is only observed in natural crystals.

At the light of values compiled in Table 2, coercivity can also be rejected as a dominant factor in the variation of initial susceptibility with field strength. Samples 8A, 4A and 4E, with the same coercivity display the three types of behaviour: type i), ii) and iii), respectively (Fig. 2).

Minor loops measurements at 77 K show most of the samples have open loops at low fields, they suffer from hysteresis, so the applied field is out of the reversible zone. However, sample 2E exemplarizes a case with linear susceptibility, but minor loops displaying hysteresis at 77 K.

Comparing results from the Day plot (Fig. 4) and initial susceptibility at 330 K and 77 K (Figs. 2 and 3), data suggest that samples with  $M_r/M_s > 0.5$  display linear or constant behaviour.

In a previous work, Guerrero-Suarez & Martín-Hernández (2012) suggested the influence of the domain structure within the basal plane as a parameter controlling of initial susceptibility behaviour in hematite natural crystals. Minor loops measurements cannot provide information about domain structure, but domain wall displacements can be recognised by abrupt changes in magnetization (Barkhausen jumps). A closer look into Figs 3 (initial susceptibility at 77 k) and 5 (Barkhausen jumps) shows that the susceptibility slope changes coincide with Barkhausen jumps. Fig. 8 displays the comparison between the initial susceptibility at 77 K, obtained by minor loops and the magnetization gradient (Barkhausen jumps) as a function of field. Sample 1A shows a non-linear initial susceptibility

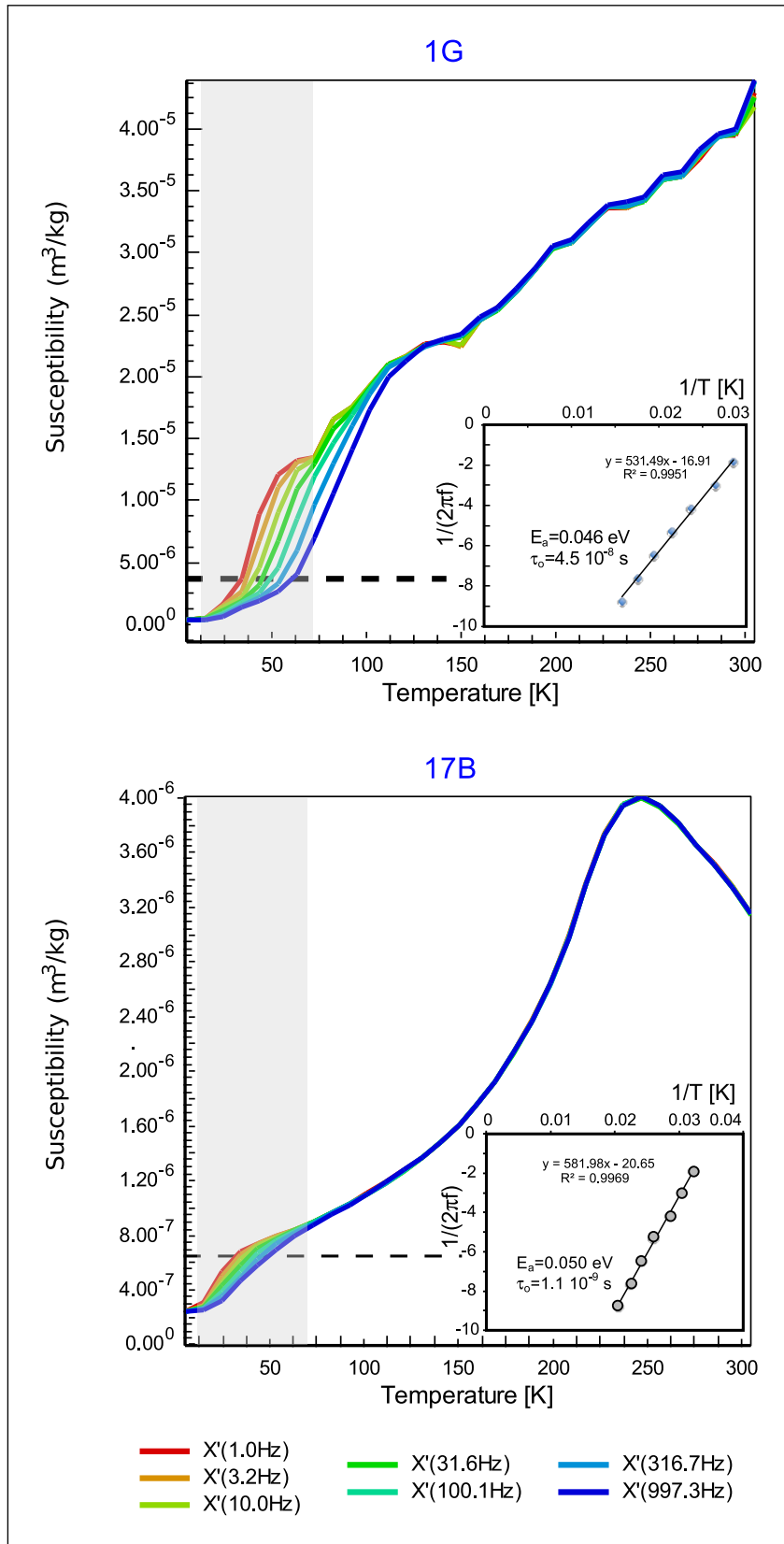


**Figure 7.** AC-susceptibility for (a) sample 1G and (b) sample 17B. Inset: Arrhenius plot, it is obtained from the temperature at which each curve crosses the dashed line.

(Fig. 8a) where susceptibility slope changes are related to large increments of magnetization (Fig. 8b). Fig. 8c corresponds to sample 17B, in this case the initial susceptibility is constant within error, and its magnetization gradient, displayed in Fig. 8d, is lower than the signal noise. In summary, Fig. 8 shows that the samples with significant jumps have non-linear initial susceptibility.

Possible mechanisms causing Barkhausen jumps are: (1) nucleation of domain walls, the creation and expansion of walls into the particle volume to produce a fully developed domain structure; and (2) bulk pinning of full-scale domain walls (Coeey 2010, 2001; Halgedahl & Fuller 1983; Menyeh & O'Reilly 1995). Thermal effects are discarded because they are not relevant for the Barkhausen effect in bulk three dimensional samples (Urbach et al. 1995). The main features of bulk pinning are high susceptibility, low coercivity and domain wall displacements at low field ( $\sim 5 - 10Oe$ ) (Halgedahl & Fuller 1983). Bulk pinning would also explain the negative slope in initial susceptibility in samples 4E and 1A, but domain nucleation cannot be excluded from these measurements. On the contrary, domain nucleation would explain the recovery magnetization in ZFC-FC curves of sample 2E above 30 K and the constant susceptibility at 77 K in samples 2E, 4N and 17B. Therefore, a combination of domain nucleation and pinning is proposed to explain the magnetization behaviour.

Samples with significant Barkhausen jumps show hysteresis phenomena at 77 K too. This magnetic moment is analyzed from ZFC-FC curves and AC-susceptibility measurements. ZFC-FC curves yield anomalous results for hematite crystals, none of the samples exhibit Morin transition. There are several reasons for Morin transition being suppressed, among the most relevant one could cite  $T_i$  or grain size. Titanium is known to suppress the transition in concentrations as low as less than 1% (Kaye 1962; Morrish 1994), and the  $TiO_2$  minimum value of our samples is 3% (Table 1). However contrary to expectations, samples with an inflection at the Morin temperature have the highest  $TiO_2$  content (Table 1, Fig. 6, left column). In this study, in most of the samples (Fig. 6 and Supplementary material) the ZFC-FC continuously increases with decreasing temperature at applied field of 2.5 T, which is characteristic from nano-systems but not from bulk materials or structures with a diameter higher than 40 nm (Luna et al. 2012; Bhowmik & Saravanan 2010). In nano-structures, remanence increase is related to surface anisotropy increase (Coeey 2010).

According to the classical Preisach model, the temperature dependence of the magnetic response below a critical temperature (e.g. the Morin transition) has two possible sources: (a) intrinsic to the system, such as the spontaneous moment and the free energy barriers or (b) extrinsic to the system, such as thermal fluctuations which reduce all of the subsystem energy barriers (Bertotti 1998). The systems with intrinsic sources are denominated anisotropy-dominated systems, and those dominated by extrinsic sources are named fluctuation-dominated systems (Song et al. 2001). The behaviour of ZFC-FC curves is different for anisotropy-dominated and fluctuation-dominated systems (Song et al. 2001).

The range of temperature where the difference between FC and ZFC is statistically significant (irreversible zone) is very low in this study, the  $T_{irr}$  value is around 20 K for many samples (except 2E, 4N and 17B), well below the temperature range at which susceptibility is low-field analyzed.

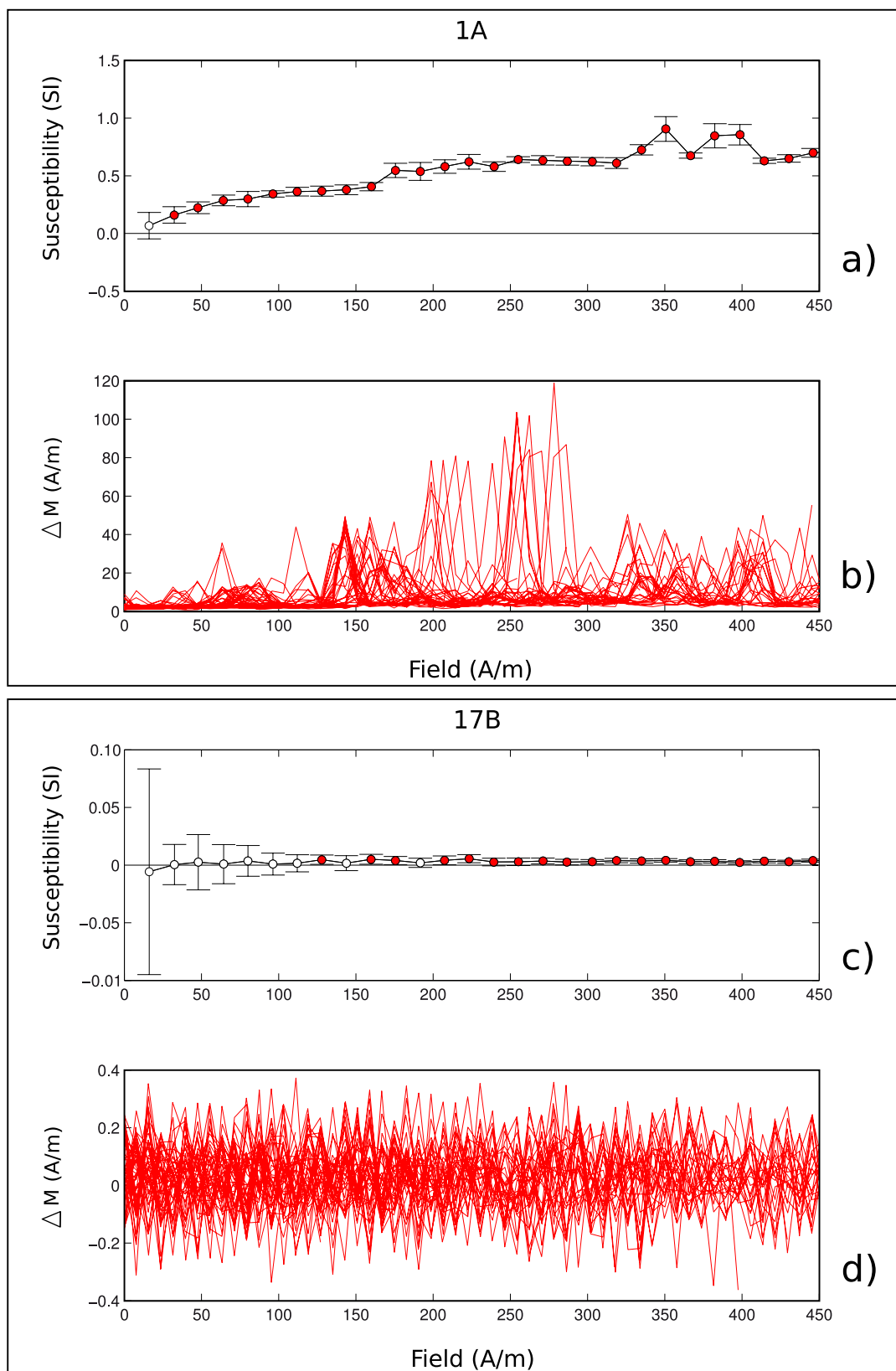


**Figure 8.** Low-field susceptibility at 77 K obtained by minor loops and Barkhausen jumps for the samples 1A and 17B.

Two mechanisms could explain the low value of the irreversible temperature, either the relaxation mechanism is the same for both FC and ZFC curve for most of the temperature range, or the applied field is high enough to saturate the irreversible effects. A closer look into the imaginary part of the AC susceptibility, which reveals the irreversible magnetization mechanism, suggests that the second mechanism (field not high enough to saturate irreversible effects) is more likely to happen. The reason for the irreversibility might be magnetic frustrations, arising from the competing ferromagnetic and antiferromagnetic exchange, besides deformed lattices and random distribution of the magnetic cations. In particular, samples 2E and 4N, which have the highest  $T_{irr}$ , have also higher coercivity at 77 K, a plateau in FC between  $T_p$  and  $T_{irr}$  (indicative of high interactions of the system) and low frequency dependence, all typical features of interactions of exchange bias type between ferromagnetic and antiferromagnetic phases (Coey 2010).

At low temperature, below 20 K, an abrupt increase of magnetization occurs and the difference between ZFC and FC is meaningful, suggesting the presence of long-range magnetic ordering. This may be due to the spin-glass like behaviour observed previously by Ishikawa et al. (1985). Moreover,  $M_{FC}$  decreases sharply with increasing temperature and there is not a plateau in low temperature (5 – 20 K), indicating the low interaction of the system (Fig. 5). ZFC curve shows a smooth inflection point around 20 K and increases at low temperature, this behaviour indicates that the system is dominated by anisotropy (Song et al. 2001). The inflection point in ZFC is attributed to some domains that do not rotate around the applied field (Fig. 5). These domains might correspond to crystallites oriented outside the basal plane. After the highest magnetization loss in ZFC-FC curves (Figs. 5 and 6), there is dispersion of susceptibility with frequency that starts at  $T_p$  (Figs. 7 and Supplementary material). The activation energy computed (Table 3) is also similar to that of superparamagnetic hematite particles (Tadić et al. 2007).

In this study, AC-susceptibility experiment has been a more sensitive tool than ZFC-FC curves to detect the Morin transition. In ZFC-FC curves, the samples exhibit a slight change around the Morin temperature, except samples 1A, 4A, 1G and 4E. In AC-susceptibility curves, the samples display a sharp inflection point in  $\chi'$  or  $\chi''$ , around the Morin temperature, except samples 1G and 4N (Morrish 1994).

## 5 CONCLUSION

The main aim of this work is to determine what property controls initial susceptibility as a function of field strength in hematite samples: grain-size, cation inclusions or domain wall displacements. The results show that:

- Known grain-size fractions, in the range of 5 – 150  $\mu\text{m}$ , display constant initial susceptibility, except for sample LHC100-150 that exhibits slight linear increase.
- Magnetic phases different to hematite, particularly  $TiO_2$ , do not show a direct correlation with the variations of initial susceptibility with increasing field.
- The changes of susceptibility slope at low-field correspond to domain wall displacements (Barkhausen jumps).
- The non-linearity of initial susceptibility increases with increasing magnetization gradient (Barkhausen jumps), obtained from minor loops. To the best of the authors' knowledge, these minor loops are the first curves that have been reported for hematite natural crystals at low temperature 77 K.
- Initial susceptibility at 300 K achieves its maximum in samples 4E and 1A, and then decreases along with the magnetic field. This behaviour may be caused by domain walls pinning.
- Almost all of the samples, except samples 2E and 4N, display ZFC-FC curves similar to nanostructures with diameter less than 40 nm. ZFC-FC magnetization and AC susceptibility have similar behaviour to acicular nanoparticles with low interactions, because the distance between particles is higher than their grain size. In-phase susceptibility, in particular, shows an activation energy in the range 20 – 90 K similar to that of hematite nanoparticles.
- All crystals show spin-glass like behaviour between 5 – 20 K and frequency-dependence in AC susceptibility for temperatures higher than 20 K.

In summary, the initial susceptibility of hematite natural crystals is controlled by domain structure, what invalidates a model that can be used to separate magnetic subfabrics mathematically as the models proposed by Hrouda (2011) for pyrrhotite and titanomagnetite. The differences observed in magnetization behaviour (ZFC-FC) may be related to the origin of magnetic interactions between ferromagnetic and antiferromagnetic phases, such as exchange bias or exchange coupling between magnetic clusters. The exchange bias would explain the behaviour of samples 2E and 4N, while Fe-rich clusters with strong intra-cluster magnetic coupling but weak inter-cluster coupling would explain the behaviour of the rest of the samples. Similar results have been reported in ilmenite-hematite solid solution ([Harrison & Redfern 2001](#)) and synthetic hematite ([Ishikawa et al. 1985](#)). But in order to verify this hypothesis, it would be useful to observe the domains with TEM, MOKE or some other imaging technique and/or rotational hysteresis determination. Also low-temperature hysteresis after field cooling is recommended.

## **ACKNOWLEDGMENTS**

This work is supported by Project no CGL2011-24790 from Spanish Ministry of Economy and Competitiveness and Visiting Research Fellowships of Institute for Rock Magnetism (IRM, University of Minnesota, USA) to SGS. We thank to Dr. Dario Bilardello and Prof. Mike Jackson from IRM for fruitful suggestions and technical assistance during the stay of SGS in the IRM. To Dr. Dekkers who kindly provided the hematite grain-sizes fractions. The manuscript has benefited from comments of two anonymous reviewers and we also acknowledge comments and suggestions of editor Professor A. Biggin.

## **APPENDIX A: SUPPLEMENTARY MATERIAL**

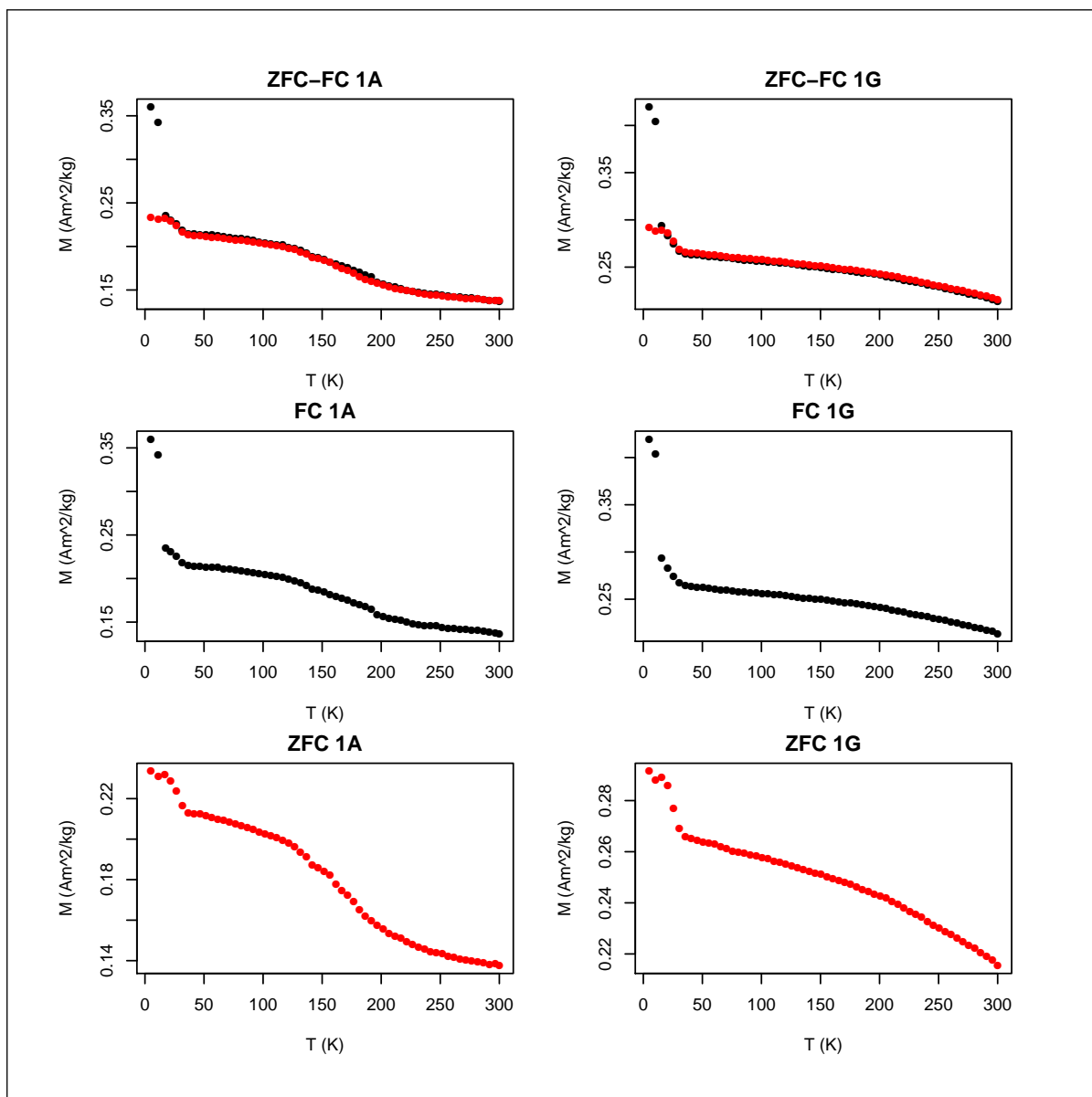


**Figure A8.** ZFC-FC from 5 to 300 K for hematite natural crystals. a) sample 1A and b) sample 1G.

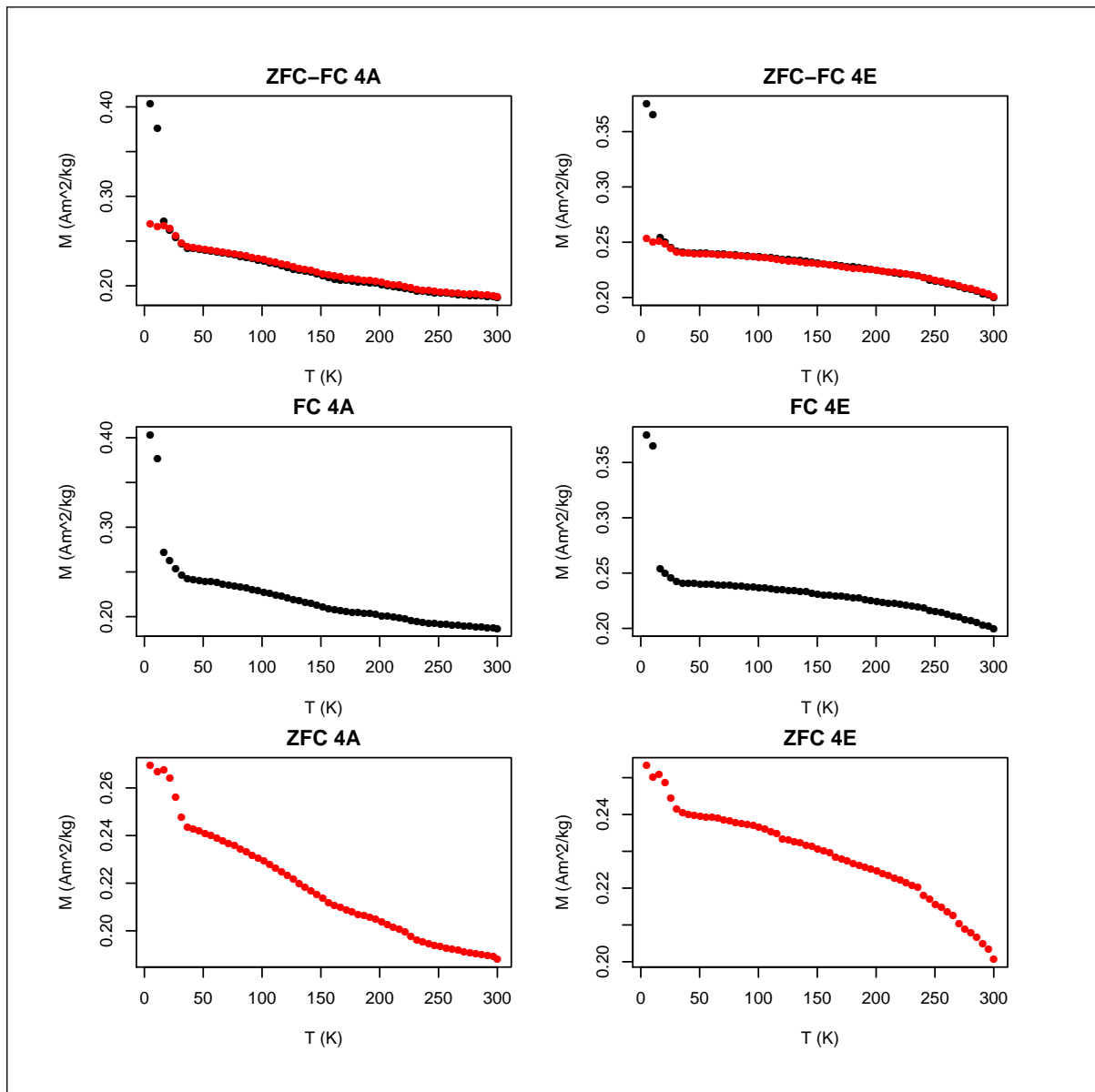
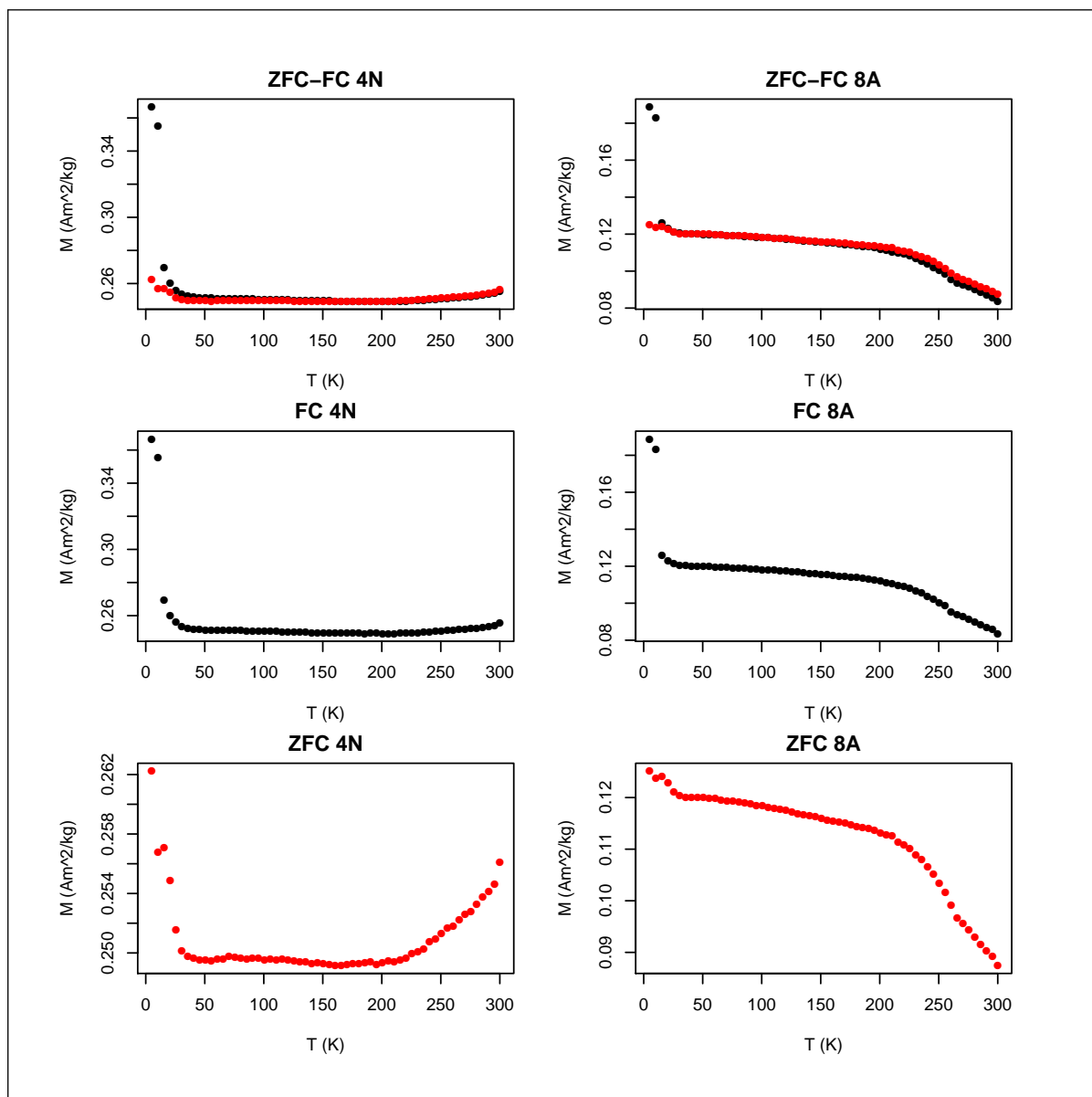


Figure A9. ZFC-FC from 5 to 300 K for hematite natural crystals. a) sample 4A and b) sample 4E.



**Figure A10.** ZFC-FC from 5 to 300 K for hematite natural crystals. a) sample 1G and b) sample 17B.

## REFERENCES

- Bertotti, G., 1998. *Hysteresis in magnetism: for physicists, materials scientists, and engineers*, Academic press.
- Bhowmik, R. & Saravanan, A., 2010. Surface magnetism, morin transition, and magnetic dynamics in antiferromagnetic  $\alpha$ -Fe<sub>2</sub>O<sub>3</sub> (hematite) nanograins, *Journal of Applied Physics*, **107**(5), 053916.
- Borradaile, G. J. & Jackson, M., 2004. Anisotropy of magnetic susceptibility (ams): magnetic petrofabrics of deformed rocks, *Geological Society, London, Special Publications*, **238**(1), 299–360.
- Bozorth, R. M., 1993. Ferromagnetism, *Ferromagnetism*, by Richard M. Bozorth, pp. 992. ISBN 0-7803-1032-2. Wiley-VCH, August 1993., **1**.
- Butler, R. F., 1992. *Paleomagnetism: magnetic domains to geologic terranes*, vol. 319, Blackwell Scientific Publications Boston.
- Christensen, P., Bandfield, J., Clark, R., Edgett, K., Hamilton, V., Hoefen, T., Kieffer, H., Kuzmin, R., Lane, M., Malin, M., et al., 2000. Detection of crystalline hematite mineralization on mars by the thermal emission spectrometer: Evidence for near-surface water, *Journal of Geophysical Research: Planets (1991–2012)*, **105**(E4), 9623–9642.
- Christensen, P., Morris, R., Lane, M., Bandfield, J., & Malin, M., 2001. Global mapping of martian hematite mineral deposits: Remnants of water-driven processes on early mars, *Journal of Geophysical Research: Planets (1991–2012)*, **106**(E10), 23873–23885.
- Church, N., Feinberg, J. M., & Harrison, R., 2011. Low-temperature domain wall pinning in titanomagnetite: Quantitative modeling of multidomain first-order reversal curve diagrams and ac susceptibility, *GEOCHEMISTRY GEOPHYSICS GEOSYSTEMS*, **12**.
- Coe, J. D., 2001. Magnetic materials, *Journal of Alloys and Compounds*, **326**(1), 2–6.
- Coe, J. M., 2010. *Magnetism and magnetic materials*, Cambridge University Press.
- Day, R., Fuller, M., & Schmidt, V., 1977. Hysteresis properties of titanomagnetites: grain-size and compositional dependence, *Physics of the Earth and Planetary Interiors*, **13**(4), 260–267.
- de Boer, C. B. & Dekkers, M. J., 2001. Unusual thermomagnetic behaviour of haematites: neoformation of a highly magnetic spinel phase on heating in air, *Geophysical Journal International*, **144**(2), 481–494.
- de Boer, C. B., Mullender, T. A., & Dekkers, M. J., 2001. Low-temperature behaviour of haematite: susceptibility and magnetization increase on cycling through the morin transition, *Geophysical Journal International*, **146**(1), 201–216.
- de Wall, H. & Worm, H.-U., 1993. Field dependence of magnetic anisotropy in pyrrhotite: effects of texture and grain shape, *Physics of the earth and planetary interiors*, **76**(1), 137–149.
- Dekkers, M. J., 1988. Some rockmagnetic parameters for natural goethite, pyrrhotite and fine-grained hematite, *Geologica Ultraiectina*, **51**, 1–249.
- Dunlop, D. & Özdemir, Ö., 2007. Magnetizations in rocks and minerals, *Treatise on Geophysics*, **5**, 277–336.
- Dunlop, D. J., 1971. Magnetic properties of fine particles hematite, *Ann. Geophys.*, **27**, 269–293.
- Dunlop, D. J. & Özdemir, Ö., 2001. *Rock magnetism: fundamentals and frontiers*, vol. 3, Cambridge University

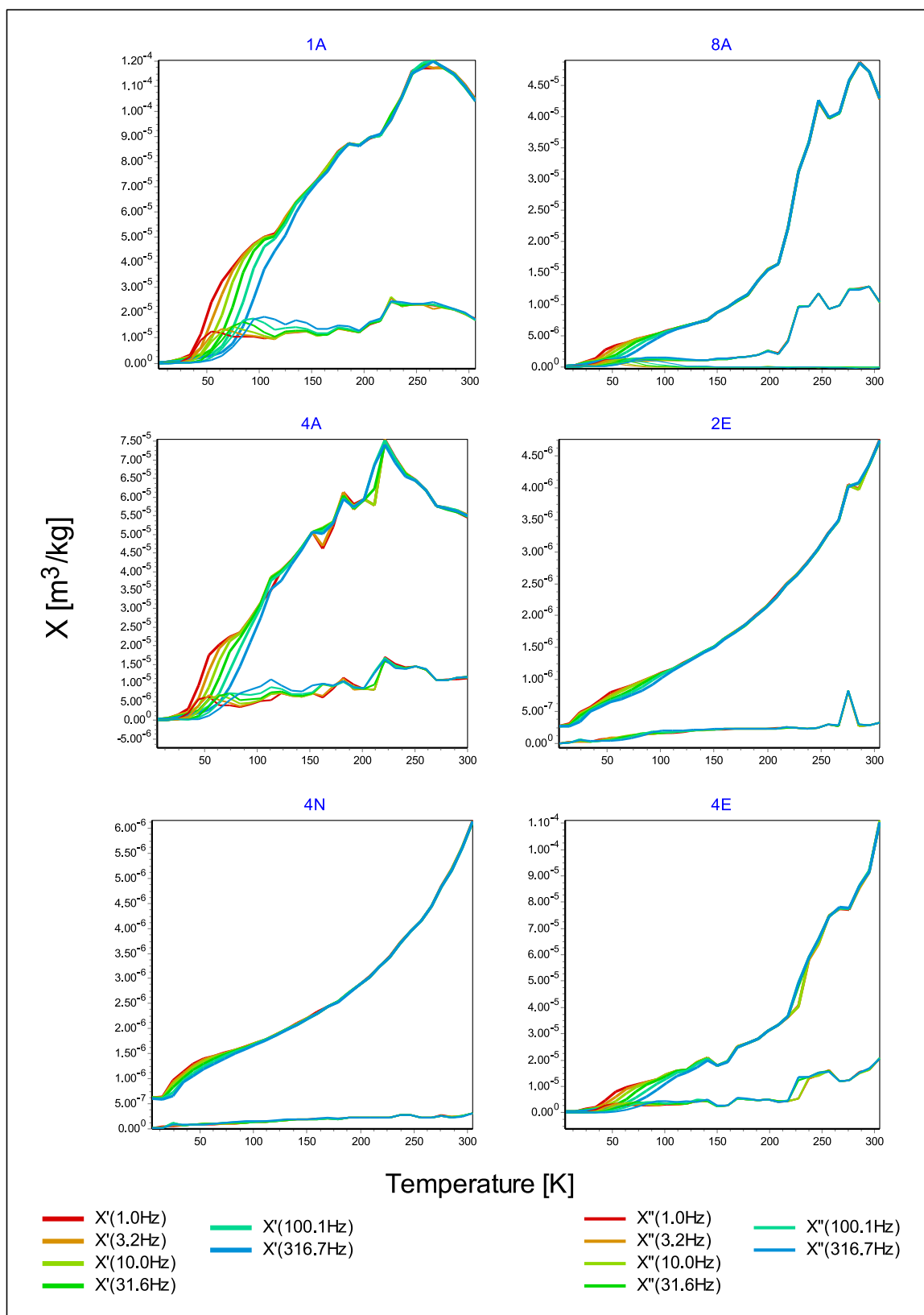


Figure A11. AC-susceptibility.

Press.

- Dzyaloshinsky, I., 1958. A thermodynamic theory of weak ferromagnetism of antiferromagnetics, *Journal of Physics and Chemistry of Solids*, **4**(4), 241–255.
- Fuller, M., 1987. 9. experimental methods in rock magnetism and paleomagnetism, *Methods of experimental Physics*, **24**, 303–471.
- Guerrero-Suarez, S. & Martín-Hernández, F., 2012. Magnetic anisotropy of hematite natural crystals: increasing low-field strength experiments, *International Journal of Earth Sciences*, **101**(3), 625–636.
- Halgedahl, S. & Fuller, M., 1983. The dependence of magnetic domain structure upon magnetization state with emphasis upon nucleation as a mechanism for pseudo-single-domain behavior, *Journal of Geophysical Research: Solid Earth (1978–2012)*, **88**(B8), 6505–6522.
- Harrison, R. & Redfern, S., 2001. Short-and long-range ordering in the ilmenite–hematite solid solution, *Physics and Chemistry of Minerals*, **28**(6), 399–412.
- Harstra, R. L., 1982. Some rock magnetic parameters for natural iron-titanium oxides, *Ph.D. thesis, State University of Utrecht*, pp. 145.
- Hrouda, F., 2002. Low-field variation of magnetic susceptibility and its effect on the anisotropy of magnetic susceptibility of rocks, *Geophysical Journal International*, **150**(3), 715–723.
- Hrouda, F., 2007. Anisotropy of magnetic susceptibility of rocks in the rayleigh law region: modelling errors arising from linear fit to non-linear data, *Studia Geophysica et Geodaetica*, **51**(3), 423–438.
- Hrouda, F., 2009. Determination of field-independent and field-dependent components of anisotropy of susceptibility through standard ams measurement in variable low fields i: Theory, *Tectonophysics*, **466**(1), 114–122.
- Hrouda, F., 2011. Anisotropy of magnetic susceptibility in variable low-fields: a review, in *The Earth's Magnetic Interior*, pp. 281–292, Springer.
- Hrouda, F. & Ježek, J., 2014. Frequency-dependent ams of rocks: A tool for the investigation of the fabric of ultrafine magnetic particles, *Tectonophysics*, **629**, 27–38.
- Hrouda, F., Chlupáčová, M., & Mrázová, Š., 2006. Low-field variation of magnetic susceptibility as a tool for magnetic mineralogy of rocks, *Physics of the Earth and Planetary Interiors*, **154**(3), 323–336.
- Ishikawa, Y., Saito, N., Arai, M., Watanabe, Y., & Takei, H., 1985. A new oxide spin glass system of  $(1-x)$   $\text{FeTiO}_3-x \text{Fe}_2\text{O}_3$ . i. magnetic properties, *Journal of the Physical Society of Japan*, **54**(1), 312–325.
- Jackson, M., Moskowitz, B., Rosenbaum, J., & Kissel, C., 1998. Field-dependence of ac susceptibility in titanomagnetites, *Earth and Planetary Science Letters*, **157**(3), 129–139.
- Kaye, G., 1962. The effect of titanium on the low temperature transition in natural crystals of haematite, *Proceedings of the Physical Society*, **80**(1), 238.
- Kletetschka, G., Wasilewski, P. J., & Taylor, P. T., 2000a. Hematite vs. magnetite as the signature for planetary magnetic anomalies?, *Physics of the Earth and Planetary Interiors*, **119**(3), 259–267.
- Kletetschka, G., Wasilewski, P. J., & Taylor, P. T., 2000b. Mineralogy of the sources for magnetic anomalies on mars, *Meteoritics & Planetary Science*, **35**(5), 895–899.
- Kletetschka, G., Ness, N. F., Connerney, J., Acuna, M., & Wasilewski, P., 2005. Grain size dependent potential

- for self generation of magnetic anomalies on mars via thermoremanent magnetic acquisition and magnetic interaction of hematite and magnetite, *Physics of the Earth and Planetary Interiors*, **148**(2), 149–156.
- Luna, C., Vega, V., Prida, V. M., & Mendoza-Reséndez, R., 2012. Morin transition in hematite nanocrystals self-assembled into three-dimensional structures, *Journal of nanoscience and nanotechnology*, **12**(9), 7571–7576.
- Martin-Hernandez, F. & Guerrero-Suárez, S., 2012. Magnetic anisotropy of hematite natural crystals: high field experiments, *International Journal of Earth Sciences*, **101**(3), 637–647.
- Martin-Hernandez, F. & Hirt, A. M., 2013. Evidence for weak ferromagnetic moment within the basal plane of hematite natural crystals at low temperature, *Geochemistry, Geophysics, Geosystems*, **14**(10), 4444–4457.
- Martín-Hernández, F., Dekkers, M., Bominaar-Silkens, I., & Maan, J., 2008. Magnetic anisotropy behaviour of pyrrhotite as determined by low-and high-field experiments, *Geophysical Journal International*, **174**(1), 42–54.
- Menyeh, A. & O'Reilly, W., 1995. The coercive force of fine particles of monoclinic pyrrhotite (Fe<sub>7</sub>S<sub>8</sub>) studied at elevated temperature, *Physics of the Earth and Planetary Interiors*, **89**(1), 51–62.
- Morin, F., 1950. Magnetic susceptibility of  $\alpha$ -Fe<sub>2</sub>O<sub>3</sub> and  $\alpha$ -Fe<sub>2</sub>O<sub>3</sub> with added titanium, *Physical Review*, **78**(6), 819.
- Moriya, T., 1960. Anisotropic superexchange interaction and weak ferromagnetism, *Physical Review*, **120**(1), 91.
- Morrish, A. H., 1994. *Canted antiferromagnetism: hematite*, World Scientific.
- Néel, L., 1953. Some new results on antiferromagnetism and ferromagnetism, *Reviews of Modern Physics*, **25**(1), 58.
- Özdemir, Ö. & Dunlop, D. J., 2005. Thermoremanent magnetization of multidomain hematite, *Journal of Geophysical Research: Solid Earth (1978–2012)*, **110**(B9).
- Özdemir, Ö. & Dunlop, D. J., 2006. Magnetic memory and coupling between spin-canted and defect magnetism in hematite, *Journal of Geophysical Research: Solid Earth (1978–2012)*, **111**(B12).
- Özdemir, Ö., Dunlop, D. J., & Berquo, T. S., 2008. Morin transition in hematite: Size dependence and thermal hysteresis, *Geochemistry, Geophysics, Geosystems*, **9**(10).
- Özdemir, Ö., Dunlop, D. J., & Jackson, M., 2009. Frequency and field dependent susceptibility of magnetite at low temperature, *Earth, planets and space*, **61**(1), 125–131.
- Peters, C. & Dekkers, M., 2003. Selected room temperature magnetic parameters as a function of mineralogy, concentration and grain size, *Physics and Chemistry of the Earth, Parts A/B/C*, **28**(16), 659–667.
- Pokorný, J., Suza, P., & Hrouda, F., 2004. Anisotropy of magnetic susceptibility of rocks measured in variable weak magnetic fields using the kly-4s kappabridge, *Geological Society, London, Special Publications*, **238**(1), 69–76.
- Pokorný, J., Suza, P., Pokorný, P., Chlupáčová, M., & Hrouda, F., 2006. Widening power of low-field magnetic methods in the investigation of rocks and environmental materials using the multi-function kappabridge set, in *Geophys. Res. Abstr.*, vol. 8.

- Song, T., Roshko, R., & Dahlberg, E. D., 2001. Modelling the irreversible response of magnetically ordered materials: a preisach-based approach, *Journal of Physics: Condensed Matter*, **13**(14), 3443.
- Tadić, M., Marković, D., Spasojević, V., Kusigerski, V., Remškar, M., Pirnat, J., & Jagličić, Z., 2007. Synthesis and magnetic properties of concentrated  $\alpha$ -Fe<sub>2</sub>O<sub>3</sub> nanoparticles in a silica matrix, *Journal of alloys and compounds*, **441**(1), 291–296.
- Tarling, D. & Hrouda, F., 1993. *Magnetic anisotropy of rocks*, Springer Science & Business Media.
- Urbach, J., Madison, R., & Markert, J., 1995. Reproducible noise in a macroscopic system: magnetic avalanches in permivar, *arXiv preprint adap-org/9508005*.
- Worm, H.-U., 1991. Multidomain susceptibility and anomalously strong low field dependence of induced magnetization in pyrrhotite, *Physics of the earth and planetary interiors*, **69**(1), 112–118.
- Worm, H.-U., Clark, D., & Dekkers, M., 1993. Magnetic susceptibility of pyrrhotite: grain size, field and frequency dependence, *Geophysical Journal International*, **114**(1), 127–137.